Helium dimer dispersion forces and correlation potentials in density functional theory

Mark J. Allen and David J. Tozer[a)]
Department of Chemistry, University of Durham, South Road, Durham DH1 3LE, United Kingdom

(Received 18 July 2002; accepted 30 September 2002)

The dispersion interaction in the helium dimer is considered from the viewpoint of the force on a nucleus. At large internuclear separations, Brueckner coupled cluster BD(T) forces agree well with near-exact dispersion forces. The atomic density distortion associated with the dispersion force is quantified by comparing the BD(T) dimer density with a superposition of atomic densities. For density functional theory calculations in the Hartree–Fock–Kohn–Sham (HFKS) formalism, the accuracy of the dispersion force is governed by the correlation potential. Calculations using the conventional Lee–Yang–Parr [Phys. Rev. B **37**, 785 (1988)] potential only generate a small density distortion, giving forces significantly smaller than BD(T). The BD(T) electron densities are therefore used to determine improved correlation potentials using a modified Zhao–Morrison–Parr (ZMP) approach [Phys. Rev. A **50**, 2138 (1994)]. HFKS calculations using these ZMP potentials quantitatively reproduce the distortion, giving dispersion forces in good agreement with BD(T). The dimer ZMP correlation potential is partitioned into two parts, one equal to the sum of two unperturbed spherical atomic correlation potentials and the other representing an interaction potential. HFKS calculations using the former do not generate the distortion; forces are close to Hartree–Fock. Calculations using the latter do generate the distortion, giving forces essentially identical to those from the full dimer potential. The origin of the distortion is traced to the asymmetric structure of the interaction correlation potential in the vicinity of each nucleus. © *2002 American Institute of Physics.* [DOI: 10.1063/1.1522715]

I. INTRODUCTION

The description of van der Waals interactions is a major challenge for density functional theory (DFT) approximations. Calculations using conventional exchange-correlation functionals have been performed for a range of systems, including rare gas dimers,[1–10] C_6H_6 dimer,[3,7,9,11] CH_4 and C_2H_2 dimers,[9,12] $He\cdots CO_2$,[13,14] N_2 dimer,[15] $C_6H_6\cdots X$ [$X=O_2$, N_2, CO (Ref. 16), Ne, Ar (Ref. 3)], and other nonbonded dimeric complexes.[17] Common conclusions are reached. The local density approximation (LDA) tends to overbind[1,2,4,5,16] while the performance of generalized gradient approximation (GGA) and hybrid functionals is sensitive to the choice of exchange approximation. Functionals based on Becke 1988 exchange[18] often predict a repulsive interaction;[1–3,5–9,11–13,15–17] those based on PW91 (Ref. 19) or PBE (Ref. 20) exchange do tend to bind, although quantitative accuracy is lacking.[4–9,14–16] This sensitivity to the exchange functional has been attributed[5,16] to the behavior of the exchange enhancement factor at large reduced density gradient s; the Becke 1988 enhancement factor diverges, whereas the PW91 and PBE factors are better behaved. In our preliminary studies, we obtained results consistent with this assessment. The HCTH93 (Ref. 21) exchange-correlation functional, whose exchange enhancement factor increases rapidly with s, does not bind the helium dimer. The 1/4 functional,[22] whose enhancement factor increases more gradually,[23] does bind. For a recent review of van der Waals studies using conventional functionals, see Ref. 24.

A DFT calculation using an appropriately chosen conventional functional can therefore provide a qualitative description of van der Waals systems at intermediate separations, where there is a non-negligible overlap between the interacting fragments and the interaction energy is composed of several terms (dispersion, exchange-dispersion, electrostatic, exchange-repulsion, etc.). At larger separations, however, where overlap is negligible, the interaction energy is dominated by the long-range dispersion energy, arising from correlated interactions between electrons on the separate fragments. The local nature of conventional functionals means they are fundamentally unable to describe this feature, failing to recover the leading $-C_6R^{-6}$ interaction energy. Although this term can be introduced in an empirical manner,[25] more advanced methods must be used to introduce it rigorously. These include long-range[26–33] and seamless[34–38] approaches; see Ref. 39 for an assessment of some of these methods. Kohn–Sham orbitals have also been used within symmetry-adapted perturbation theory.[40,41]

In this study we consider the long-range dispersion interaction in DFT from the viewpoint of the force on a nucleus, rather than from the usual viewpoint of the electronic energy. Given that dispersion is a correlation effect, we treat exchange exactly using the Hartree–Fock–Kohn–Sham (HFKS) formalism.[42,43] The electronic energy is written

$$E_{\mathrm{DFT}}=E_{\mathrm{HF}}[\{\varphi_i\}]+E_{\mathrm{C}}[\rho], \tag{1}$$

a)Fax: 0191 384 4737; Electronic mail: D.J.Tozer@Durham.ac.uk

where $E_{\mathrm{HF}}[\{\varphi_i\}]$ is the Hartree–Fock functional, $E_{\mathrm{C}}[\rho]$ is an approximate correlation energy functional, and $\rho(\mathbf{r})$ is the electron density

$$\rho(\mathbf{r})=\sum_i \varphi_i^2(\mathbf{r}). \tag{2}$$

Expansion of the orbitals $\{\varphi_i\}$ in a basis set $\{\eta_\beta\}$ allows the HFKS equations

$$\int F_{\mathrm{HF}}(\mathbf{r},\mathbf{r}')\varphi_i(\mathbf{r}')d\mathbf{r}'+v_{\mathrm{C}}(\mathbf{r})\varphi_i(\mathbf{r})-\epsilon_i\varphi_i(\mathbf{r})=0 \tag{3}$$

to be recast as secular equations

$$\sum_\beta \int \eta_\alpha(\mathbf{r})\Bigg[\int F_{\mathrm{HF}}(\mathbf{r},\mathbf{r}')\,\eta_\beta(\mathbf{r}')d\mathbf{r}'+v_{\mathrm{C}}(\mathbf{r})\,\eta_\beta(\mathbf{r}) - \epsilon_i\,\eta_\beta(\mathbf{r})\Bigg]d\mathbf{r}C_{\beta i}=0, \tag{4}$$

where $F_{\mathrm{HF}}(\mathbf{r},\mathbf{r}')$ is the coordinate representation of the Hartree–Fock operator (nonmultiplicative due to orbital exchange) and

$$v_{\mathrm{C}}(\mathbf{r})=\frac{\delta E_{\mathrm{C}}[\rho]}{\delta\rho(\mathbf{r})} \tag{5}$$

is the correlation potential. The HFKS force on nucleus A is then

$$\mathbf{F}_{\mathrm{DFT}}=-\frac{\partial E_{\mathrm{DFT}}}{\partial\mathbf{R}_{\mathrm{A}}}=-E_{\mathrm{HF}}^{\mathbf{R}_{\mathrm{A}}}[\{\varphi_i\}]-\int\rho^{\mathbf{R}_{\mathrm{A}}}(\mathbf{r})v_{\mathrm{C}}(\mathbf{r})d\mathbf{r} + \sum_i \epsilon_i S_{ii}^{\mathbf{R}_{\mathrm{A}}}, \tag{6}$$

where $E_{\mathrm{HF}}^{\mathbf{R}_{\mathrm{A}}}[\{\varphi_i\}]$, $\rho^{\mathbf{R}_{\mathrm{A}}}(\mathbf{r})$, and $S_{ii}^{\mathbf{R}_{\mathrm{A}}}$ are the basis-function-only derivatives of the Hartree–Fock functional, density, and orbital overlap matrix, respectively, with respect to the nuclear coordinate vector $\mathbf{R}_{\mathrm{A}}$. Other than $v_{\mathrm{C}}(\mathbf{r})$, all the quantities in Eq. (6) can be constructed from the solutions to Eq. (4). Given that $v_{\mathrm{C}}(\mathbf{r})$ is the only approximated term in Eq. (4), it follows that the quality of this potential alone determines the quality of the force for a given basis set. In essence, $E_{\mathrm{C}}[\rho]$ governs the accuracy of the total energy, so its functional derivative governs the energy derivative. This dependence on $v_{\mathrm{C}}(\mathbf{r})$ is particularly evident when the basis set is complete, since Eq. (6) reduces to the Hellmann–Feynman force.[44] For a given Born–Oppenheimer configuration, this depends only on the density, whose accuracy is governed by $v_{\mathrm{C}}(\mathbf{r})$ through Eqs. (2) and (3).

At large separation, the force on a nucleus in a van der Waals molecule is almost exclusively due to the dispersion interaction. To describe this dispersion force accurately within the HFKS formalism therefore requires an accurate representation of $v_{\mathrm{C}}(\mathbf{r})$ at large separation; integration of this force along the dissociation path yields the dispersion interaction energy. We regard $v_{\mathrm{C}}(\mathbf{r})$ as a key quantity, containing essential physics of DFT dispersion. The aim of this study is to use *ab initio* electron densities to learn about the structure of $v_{\mathrm{C}}(\mathbf{r})$ and its relationship to dispersion forces in the helium dimer He_2.

We commence in Sec. II by providing computational details and choosing internuclear separations in He_2 where dispersion dominates. The physical origin of the dispersion force—a distortion of the atomic densities—is discussed and quantified using BD(T) densities. Deficiencies with conventional correlation potentials are highlighted by considering HFKS forces using the Lee–Yang–Parr (LYP) potential.[45] Correlation potentials are then determined directly from the BD(T) electron densities, using a modified Zhao–Morrison–Parr (ZMP) (Ref. 46) approach. Self-consistent HFKS calculations are performed using these potentials and forces are determined. The partitioning of the correlation potential into atomic and interaction components is investigated. Conclusions are presented in Sec. III.

II. RESULTS

A. Computational details

All calculations were performed using a modified version of the CADPAC program[47] with an extensive $7s5p4d$ basis set on the He atoms, corresponding to the nuclear centred part of the DC^+BS (Dc147) basis set of Ref. 48, with the f functions removed for technical reasons. Unless otherwise stated, the BD(T), Hartree–Fock, and DFT forces were all evaluated analytically, using conventional rigorous energy derivative expressions. Where possible, numerical stability was confirmed by comparing the analytic forces with numerical forces determined from energies at perturbed geometries. Basis set superposition errors (BSSE) affect the shape of the interaction energy curve and so also affect the calculated forces. All forces were corrected for BSSE by differentiating the counterpoise energy correction. This requires the force on a single helium atom, calculated in the presence of additional ghost atom basis functions. For DFT calculations, the integration grid on the ghost atom was also included, in order to account for integration grid superposition error. Given our extensive basis set, large internuclear separations, and near-saturated integration grids, the BSSE corrections to the total forces are very small. To the number of decimal places quoted they are negligible for all methods except BD(T) [where it contributes 0.1×10^{-6} a.u. (about 2%) to the forces at 8.0 and 8.5 a.u.]. BSSE corrections to Hellmann–Feynman forces were slightly larger.

All BD(T) densities are relaxed densities. HFKS correlation potentials were determined from these densities using the methodology of Refs. 49 and 50, which is a modification of the ZMP approach,[46] based on the constrained search formulation.[51] The method is as follows. The only terms in Eq. (1) that are not explicit functionals of the density are the noninteracting kinetic and orbital exchange energies in $E_{\mathrm{HF}}[\{\varphi_i\}]$. Minimization of the sum of these two terms with respect to the orbitals, subject to the constraint that the density equals the BD(T) density, gives the HFKS orbitals associated with that density. The addition of appropriate explicit density functionals to the minimization ensures that the resulting one-electron equations take the same form as Eq. (3), but does not change the solution. Comparison of the equations then allows $v_{\mathrm{C}}(\mathbf{r})$ to be identified in terms of the BD(T) density, the iterating density, and a Lagrange multi-

plier λ associated with the density constraint. The one-electron equations are solved within a basis set framework and the potential is tabulated numerically on a DFT numerical integration grid.

The Lagrange multiplier λ is formally infinite, although for finite basis sets the BD(T) densities cannot be reproduced exactly and so this is inappropriate.[52] We considered three approaches to circumvent this problem. We considered a finite value of $\lambda=900$, as was used in Ref. 49 and in studies of exchange-correlation potentials. We also considered two extrapolation schemes. The first, from Ref. 53, involves an expansion from λ^{-3} to λ^{+1}, where the latter term represents basis set incompleteness. The second extrapolation, similar to that in Ref. 46, replaces this basis set term with λ^{-4}. To choose an optimal scheme, we used the fact that the ZMP iterating density should equal the BD(T) density, and so Hellmann–Feynman forces from the two should be identical. Comparison of the forces led us to conclude that the first extrapolation scheme did not work well; a similar conclusion was reached in Ref. 49. Forces from $\lambda=900$ were close to those from the second extrapolation scheme and so for simplicity we use a finite value of $\lambda=900$ throughout.

In all calculations, He_2 is oriented along the z axis. The nuclei, which are labeled A and B to distinguish them, are positioned at z coordinates z_A and z_B, respectively, where $z_B>z_A$ and the internuclear separation is $R=z_B-z_A$. All quoted forces correspond to the force on nucleus A. This acts along the z axis and is equal and opposite to the force on nucleus B. (Forces constructed using approximate ZMP potentials do not generally satisfy this translational invariance condition because the potentials are not exact functional derivatives. The homonuclear nature of He_2 ensures that this condition is satisfied in the present study.) A positive force pulls nucleus A towards nucleus B and so represents an attraction; a negative force is a repulsion.

B. Dispersion forces and the atomic density distortion

Our first task is to choose a set of internuclear separations R, where the interaction is dominated by dispersion. Korona *et al.*[48] fitted an accurate symmetry-adapted perturbation theory (SAPT) interaction energy for He_2 to the form

$$E_{\mathrm{SAPT}}=Ae^{-\alpha R+\beta R^2}-\sum_{n=3}^{8} f_{2n}(R,b)\frac{C_{2n}}{R^{2n}}, \tag{7}$$

where all parameters are defined in Ref. 48. At large R, this approaches the long-range dispersion energy

$$E_{\mathrm{disp}}=-\sum_{n=3}^{8}\frac{C_{2n}}{R^{2n}}=-\frac{C_6}{R^6}-\frac{C_8}{R^8}-\cdots-\frac{C_{16}}{R^{16}}. \tag{8}$$

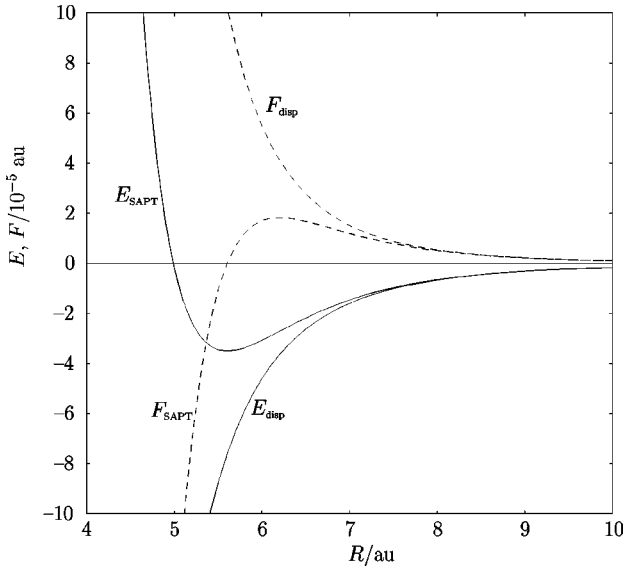

FIG. 1. SAPT interaction energy E_{SAPT} and force F_{SAPT}, together with long-range dispersion contributions E_{disp} and F_{disp} for He_2.

The force on nucleus A is

$$F_{\mathrm{SAPT}}=-\frac{\partial E_{\mathrm{SAPT}}}{\partial z_A}=\frac{\partial E_{\mathrm{SAPT}}}{\partial R}, \tag{9}$$

which at large R approaches the long-range dispersion force

$$\begin{aligned}F_{\mathrm{disp}}&=-\frac{\partial E_{\mathrm{disp}}}{\partial z_A}=\frac{\partial E_{\mathrm{disp}}}{\partial R}\\&=\sum_{n=3}^{8}\frac{2nC_{2n}}{R^{2n+1}}\\&=\frac{6C_6}{R^7}+\frac{8C_8}{R^9}+\cdots+\frac{16C_{16}}{R^{17}}.\end{aligned} \tag{10}$$

Figure 1 presents E_{SAPT} and F_{SAPT} as a function of R. Here E_{disp} and F_{disp} are also presented in order to estimate the distance where the SAPT terms reduce to these limiting long-range forms. The curves become indistinguishable beyond $R=7.5$ a.u. and so we shall concentrate on $R=8.0$, 8.5, and 9.0 a.u. Table I presents F_{disp} and F_{SAPT} at the three R values. The small difference between the two forces reflects the nonvanishing atomic overlap. We regard F_{SAPT} as near-exact reference forces.

Before presenting forces from approximate electronic structure methods, it is informative to consider the physical

TABLE I. The force on nucleus A in He_2, in units of $\times10^{-6}$ a.u., for internuclear separations $R=8.0$, 8.5, and 9.0 a.u. All forces act along the He–He bond axis. A positive force represents an attraction between the nuclei.

R	F_{disp}	F_{SAPT}	F_{HF}	$F_{\mathrm{BD(T)}}$	$F_{\mathrm{DFT}}[v^{\mathrm{dimer}}_{\mathrm{C,LYP}}]$	$F_{\mathrm{DFT}}[v^{\mathrm{dimer}}_{\mathrm{C,ZMP}}]$	$F_{\mathrm{DFT}}[v^{\mathrm{atoms}}_{\mathrm{C,ZMP}}]$	$F_{\mathrm{DFT}}[v^{\mathrm{int}}_{\mathrm{C,ZMP}}]$
8.0	5.4	5.1	−0.2	4.9	0.9	4.8	−0.3	4.8
8.5	3.4	3.3	−0.1	3.1	0.3	3.2	−0.1	3.2
9.0	2.2	2.2	−0.0	2.1	0.1	2.1	−0.0	2.1

origin of the dispersion force in the exact He_2. The electrostatic theorem of Feynman[44]—obtained by applying the differential Hellmann–Feynman theorem to a nuclear perturbation—states that the force on a nucleus is just the classical electrostatic force exerted by the other nuclei and the electron density. For He_2, the exact force on nucleus A is then

$$F = -\frac{4}{R^2} + 2\int \frac{\rho(\mathbf{r}_1)}{r_{A1}^3} z_{A1} d\mathbf{r}_1, \tag{11}$$

where the first term is the repulsive force due to nucleus B and the second is the force due to the exact density. At large R, correlation between electrons on the two atoms causes the atomic densities to be distorted towards one another. The force due to the density then pulls nucleus A in the direction of nucleus B more strongly than they repel one another, resulting in a net attractive force. Feynman described this distortion:

"*The Schrödinger perturbation theory for two interacting atoms at a separation R, large compared to the radii of the atoms, leads to the result that the charge distribution of each is distorted from central symmetry, a dipole moment of order* $1/R^7$ *being induced in each atom. The negative charge distribution of each atom has its center of gravity moved slightly toward the other.*"

Feynman also conjectured that the leading term in the dispersion force on a nucleus arose entirely from the attraction of that nucleus to its *own* distorted density. For He_2, this implies that the R^{-7} component of the force on nucleus A arises from atom A's density contribution to the second term in Eq. (11); this density is polarized towards atom B and so pulls nucleus A in that direction. Although atom B causes the dispersion force on nucleus A, its density and nucleus only explicitly contribute to the higher-order forces. Feynman's conjecture was verified by Hirschfelder and Eliason[54] for two hydrogen atoms. A general proof has been provided by Hunt;[55] see Refs. 56–58 for further discussion.

In an approximate electronic structure calculation the electrostatic theorem does not hold exactly, due to finite basis sets or nonvariational methodology. Nevertheless, we do find that all our Hartree–Fock, BD(T), and DFT forces are very close to the Hellmann–Feynman forces (11) calculated using their respective densities, demonstrating that the forces in these methods can be rationalized in terms of simple electrostatics; the force reflects the density distortion produced by the method. We shall quantify the distortion using the function $\Delta\rho(\mathbf{r})$, defined as the density of the dimer minus the sum of two isolated atomic densities, positioned at the dimer nuclear coordinates; ghost atoms are not included in the atomic calculations since the isolated atoms must be spherical. A positive $\Delta\rho(\mathbf{r})$ corresponds to a region where the density increases upon dimer formation; a negative value corresponds to a density decrease.

Table I presents forces from Hartree–Fock and BD(T), denoted F_{HF} and $F_{BD(T)}$, respectively. The former are small, repulsive, and vanish as overlap reduces; the latter are in reasonable quantitative agreement with the near-exact values. The absence of electron correlation in Hartree–Fock means that the only distortion is due to overlap (exchange)

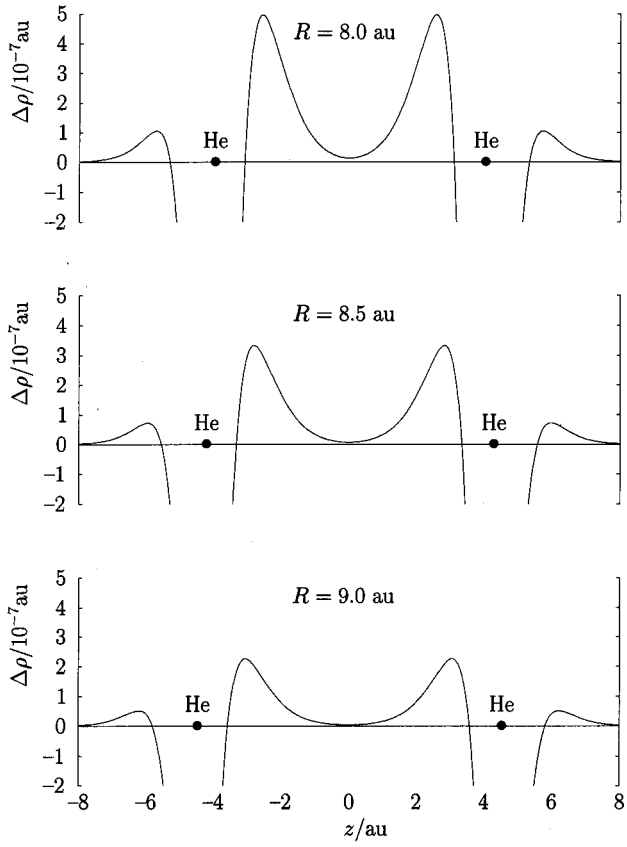

FIG. 2. Density differences $\Delta\rho(\mathbf{r})$ determined from BD(T) densities, plotted along the He–He bond axis for the three R values. The nuclei are symmetrically placed either side of $z=0$.

effects, which distorts the atomic densities *away* from one another.[59,60] The attractive force due to the density is then smaller than the nuclear repulsion, resulting in a net repulsive force. The small overlap at these large R values means this distortion—and hence the force—is very small. We do not present plots of $\Delta\rho(\mathbf{r})$ for Hartree–Fock since it can be difficult to distinguish the distortion from the numerical noise in the calculations—the Hartree–Fock dimer is essentially two spherical atoms at these large separations. By contrast, electron correlation in BD(T) distorts the atomic densities towards one another as in the exact case, overcoming the small exchange distortion. This is demonstrated in Fig. 2 where $\Delta\rho(\mathbf{r})$ for BD(T) is plotted along the He–He bond axis for the three R values. At the nuclei, the plots approach -182, -126, and -88×10^{-7} a.u. for $R=8.0$, 8.5, and 9.0 a.u., respectively, which are not visible on the scale. On either side of each nucleus, $\Delta\rho(\mathbf{r})$ exhibits a positive peak, which is much more pronounced on the side of the nucleus nearest to the other atom. Analogous plots have been presented for H_2 (Ref. 57); further discussion on the density of rare gas dimers can be found in Ref. 61. The quality of the BD(T) density is quantified by calculating the associated Hellmann–Feynman forces. For $R=8.0$, 8.5, and 9.0 a.u., the forces are $+4.8$, $+3.2$, and $+2.1\times10^{-6}$ a.u., which are close to the near-exact values of Table I.

We next consider forces from HFKS calculations. The

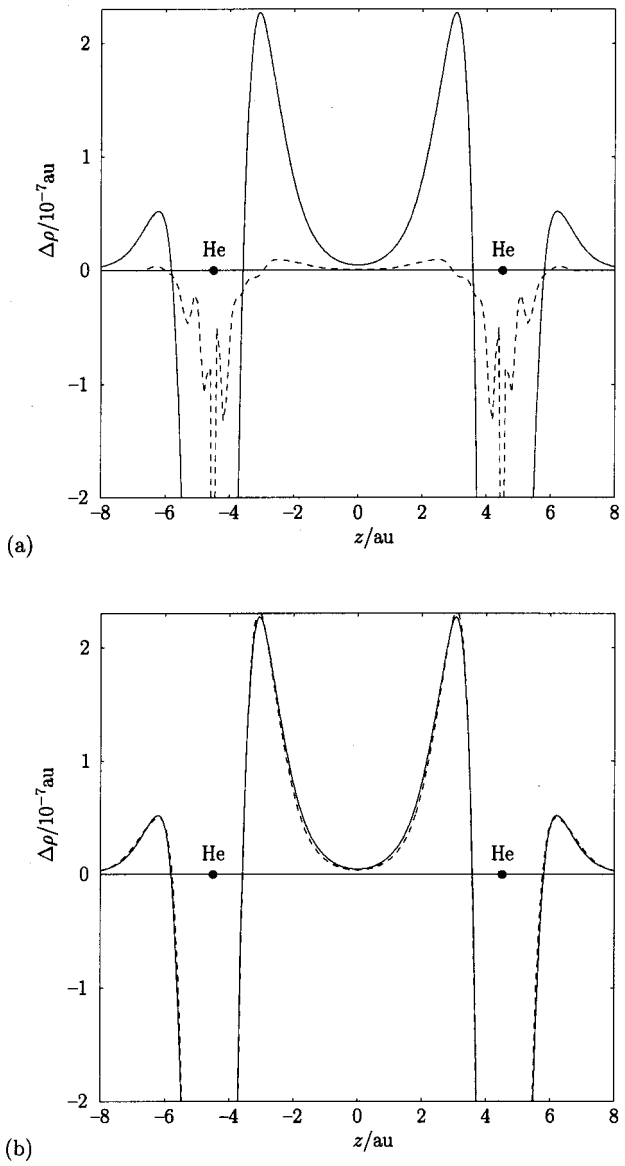

FIG. 3. Density differences $\Delta\rho(\mathbf{r})$ determined from BD(T) densities (solid line), plotted along the He–He bond axis for $R=9.0$ a.u., compared with $\Delta\rho(\mathbf{r})$ from HFKS calculations (dashed lines) using (a) LYP and (b) ZMP potentials.

only difference between the Hartree–Fock equations and the HFKS equations is the correlation potential $v_C(\mathbf{r})$. The accuracy of the HFKS forces will depend on how well this potential reproduces the density distortion.

C. DFT forces and correlation potentials

We first consider HFKS calculations using the regular LYP correlation functional. Equation (4) was solved using $v_C(\mathbf{r})=v^{\text{dimer}}_{\text{C,LYP}}(\mathbf{r})$, where $v^{\text{dimer}}_{\text{C,LYP}}(\mathbf{r})$ is the LYP potential of the dimer obtained by applying Eq. (5) to the LYP energy functional. The forces (6), denoted $F_{\text{DFT}}[v^{\text{dimer}}_{\text{C,LYP}}]$, are presented in Table I. They are attractive, which is consistent with previous observations,[10] but they are considerably smaller than those of BD(T), vanishing as overlap reduces. This failure is clearly evident in Fig. 3(a), where $\Delta\rho(\mathbf{r})$ determined from LYP HFKS densities is compared with that from BD(T), at $R=9.0$ a.u. The atomic densities are slightly distorted towards one another, but the magnitude of the distortion is significantly too small.

To improve the HFKS forces the correlation potential must be improved. We have therefore used the BD(T) dimer densities as input to our amended ZMP procedure. The calculated dimer correlation potentials are denoted $v^{\text{dimer}}_{\text{C,ZMP}}(\mathbf{r})$. To determine the associated forces, $v^{\text{dimer}}_{\text{C,ZMP}}(\mathbf{r})$ was calculated on numerical integration grids, for the three R values, and written to disk. HFKS calculations were then performed, but rather than using a conventional correlation potential, the ZMP potential was read from disk: i.e., we solve Eq. (4) using $v_C(\mathbf{r})=v^{\text{dimer}}_{\text{C,ZMP}}(\mathbf{r})$. The equations were converged to self-consistency; the resulting orbitals and eigenvalues then agree, to within negligible numerical integration error, with those from the ZMP calculation. These orbitals and eigenvalues, together with $v^{\text{dimer}}_{\text{C,ZMP}}(\mathbf{r})$, were then used to assemble the force (6). We realize that this expression is only strictly valid when the orbitals and eigenvalues are variationally optimized; however, previous studies of magnetic properties have demonstrated the practicality of evaluating variational expressions with ZMP quantities.[62] The forces determined from self-consistent calculations using $v^{\text{dimer}}_{\text{C,ZMP}}(\mathbf{r})$ are denoted $F_{\text{DFT}}[v^{\text{dimer}}_{\text{C,ZMP}}]$ and are presented in Table I.

The forces are in good agreement with $F_{\text{BD(T)}}$, quantitatively describing the dispersion force. By construction, a HFKS calculation using the ZMP potential gives a density close to BD(T). It follows that the HFKS calculations reproduce the atomic density distortion, giving high-quality forces. Figure 3(b) presents $\Delta\rho(\mathbf{r})$ calculated from HFKS densities using $v^{\text{dimer}}_{\text{C,ZMP}}(\mathbf{r})$ for the dimer and the analogous atomic ZMP potential for the atoms. The plot is almost indistinguishable from that of BD(T). The similarity between the HFKS and BD(T) densities is quantified by comparing their Hellmann–Feynman forces. The HFKS forces are $+4.5$, $+3.0$, and $+2.0\times10^{-6}$ a.u. for $R=8.0$, 8.5, and 9.0 a.u., respectively, compared to the BD(T) values of $+4.8$, $+3.2$, and $+2.1\times10^{-6}$ a.u.

Figure 4 presents $v^{\text{dimer}}_{\text{C,ZMP}}(\mathbf{r})$, plotted along the He–He bond axis for the three R values. The only discernible difference between the three plots is the increased separation between the atomic features. Figure 5 compares $v^{\text{dimer}}_{\text{C,ZMP}}(\mathbf{r})$ and $v^{\text{dimer}}_{\text{C,LYP}}(\mathbf{r})$ at $R=9$ a.u.; they bear minimal resemblance to one another. Previous studies have demonstrated significant discrepancies between approximate and near-exact correlation potentials in systems such as the helium[63] and neon[49] atoms.

D. Partitioning the correlation potential

It is important to understand why $v^{\text{dimer}}_{\text{C,ZMP}}(\mathbf{r})$ correctly distorts the atomic densities. On the scale of Fig. 4, $v^{\text{dimer}}_{\text{C,ZMP}}(\mathbf{r})$ is indistinguishable from the sum of two atomic correlation potentials. This leads us to partition the dimer potential into two terms

$$v^{\text{dimer}}_{\text{C,ZMP}}(\mathbf{r})=v^{\text{atoms}}_{\text{C,ZMP}}(\mathbf{r})+v^{\text{int}}_{\text{C,ZMP}}(\mathbf{r}). \tag{12}$$

Here $v^{\text{atoms}}_{\text{C,ZMP}}(\mathbf{r})$ is the sum of two independent atomic ZMP correlation potentials positioned at the dimer nuclear coordinates, each determined from a BD(T) atomic density.

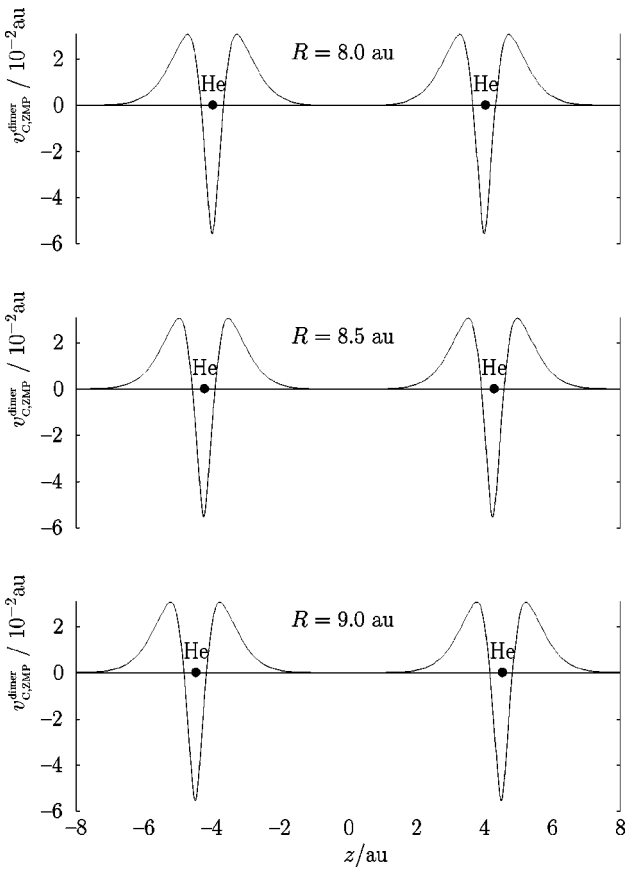

FIG. 4. Correlation potentials $v^{\rm dimer}_{\rm C,ZMP}(\mathbf{r})$ plotted along the He–He bond axis for the three R values.

$v^{\rm int}_{\rm C,ZMP}(\mathbf{r})$ is an interaction correlation potential, representing the change in the correlation potential that occurs when the atoms interact.

To determine $v^{\rm atoms}_{\rm C,ZMP}(\mathbf{r})$ on the dimer integration grid, an atomic ZMP calculation, based on a BD(T) density, was performed on atom A, with atom B included as a ghost atom with an associated numerical integration grid, but no basis functions. The calculation was repeated for atom B and the two potentials were added. The potential was input to HFKS calculations; i.e., we solve Eq. (4) using $v_{\rm C}(\mathbf{r}) = v^{\rm atoms}_{\rm C,ZMP}(\mathbf{r})$. The forces (6), denoted $F_{\rm DFT}[v^{\rm atoms}_{\rm C,ZMP}]$, are presented in Table I.

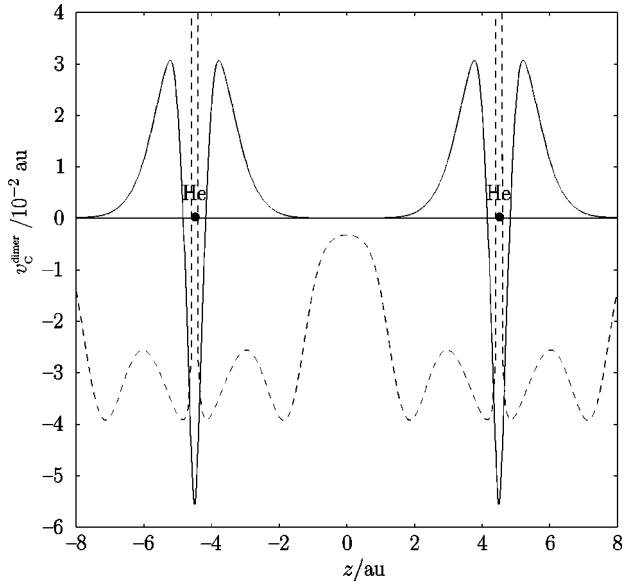

FIG. 5. Correlation potentials $v^{\rm dimer}_{\rm C,ZMP}(\mathbf{r})$ (solid curve) and $v^{\rm dimer}_{\rm C,LYP}(\mathbf{r})$ (dashed curve), plotted along the He–He bond axis for $R = 9.0$ a.u.

The forces are small and repulsive, very close to the Hartree–Fock forces. This is because the ZMP correlation potential of an isolated helium atom is short ranged. In the vicinity of each nucleus, $v^{\rm atoms}_{\rm C,ZMP}(\mathbf{r})$ is essentially a spherical atomic potential because the contribution from the potential on the other atom is so small. $v^{\rm atoms}_{\rm C,ZMP}(\mathbf{r})$ introduces correlation appropriate for isolated atoms, but does not cause the atomic densities to be distorted towards one another; we have confirmed this by examining $\Delta\rho(\mathbf{r})$ plots. The exchange distortion dominates, giving a repulsive force. In essence, a HFKS calculation using $v^{\rm atoms}_{\rm C,ZMP}(\mathbf{r})$ generates two BD(T)-like atoms that have an exchange, but no dispersion interaction.

The dispersion force therefore arises due to $v^{\rm int}_{\rm C,ZMP}(\mathbf{r})$, which is the subtle difference between $v^{\rm dimer}_{\rm C,ZMP}(\mathbf{r})$ and $v^{\rm atoms}_{\rm C,ZMP}(\mathbf{r})$. To demonstrate this we have performed HFKS calculations using just $v^{\rm int}_{\rm C,ZMP}(\mathbf{r})$ as the correlation potential; i.e., we solve Eq. (4) using $v_{\rm C}(\mathbf{r}) = v^{\rm int}_{\rm C,ZMP}(\mathbf{r})$. The forces (6), denoted $F_{\rm DFT}[v^{\rm int}_{\rm C,ZMP}]$, are presented in Table I. To the precision quoted, they are indistinguishable from those obtained with the full dimer potential. By examining $\Delta\rho(\mathbf{r})$ plots, we have confirmed that $v^{\rm int}_{\rm C,ZMP}(\mathbf{r})$ alone quantitatively reproduces the atomic density distortion.

The reason why $v^{\rm int}_{\rm C,ZMP}(\mathbf{r})$ generates the distortion is clear from Fig. 6, where the potential is plotted for the three R values; note the smaller scale compared to Fig. 4. For each plot, the potential is asymmetric in the vicinity of each nucleus. It reduces in moving from the far side to the near side of each nucleus and so shifts density to the near side, distorting the atomic densities towards one another. The potentials were calculated by subtracting two approximate ZMP potentials, so we cannot be sure that all features are quantitatively accurate; for example, the oscillatory behavior near the nuclei is sensitive to the basis set and other convergence criteria. However, the general structure is not sensitive to precise computational details.

Despite giving essentially identical dispersion forces, HFKS calculations using $v^{\rm int}_{\rm C,ZMP}(\mathbf{r})$ and $v^{\rm dimer}_{\rm C,ZMP}(\mathbf{r})$ are fundamentally different. At large R,

$$\lim_{R\to\infty} v^{\rm int}_{\rm C,ZMP}(\mathbf{r}) = 0, \tag{13}$$

but

$$\lim_{R\to\infty} v^{\rm dimer}_{\rm C,ZMP}(\mathbf{r}) = v^{\rm atoms}_{\rm C,ZMP}(\mathbf{r}), \tag{14}$$

and so, asymptotically, the former yields two Hartree–Fock atoms whereas the latter yields two BD(T)-like atoms. Quantitatively similar dispersion forces can therefore be obtained through a minor distortion of Hartree–Fock or BD(T)-like atoms. It is the distortion that matters, not the underlying atom.

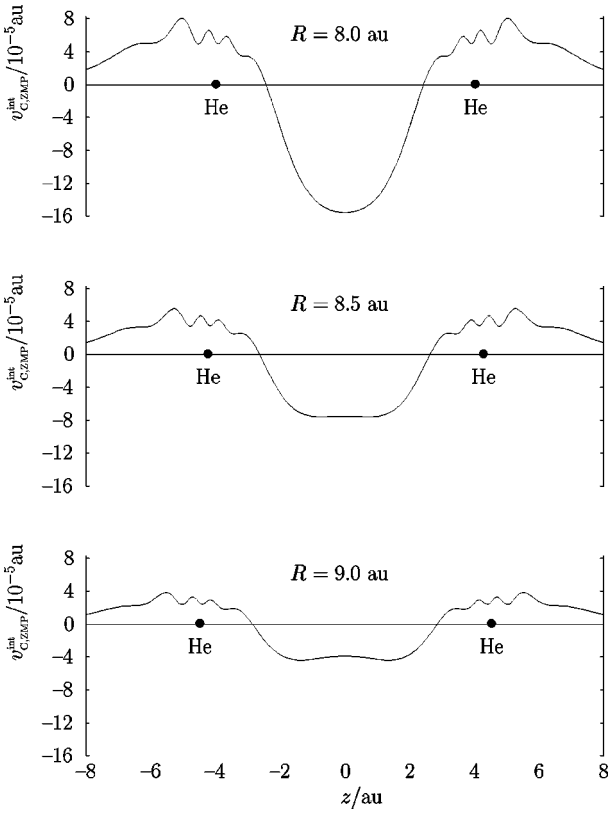

FIG. 6. Interaction correlation potentials $v^{int}_{C,ZMP}(\mathbf{r})$ plotted along the He–He bond axis for the three R values.

III. CONCLUSIONS

The dispersion interaction has been considered from the viewpoint of the force on a nucleus. When the HFKS method is used to implement this viewpoint, the key to an accurate dispersion force is an accurate correlation potential at large internuclear separation; this contrasts conventional approaches, which tend to focus on the correlation energy rather than the potential. We have used coupled-cluster BD(T) electron densities to investigate the potential and its relationship to dispersion forces in the helium dimer.

BD(T) dispersion forces are in good agreement with near-exact values. The BD(T) densities have been used to quantify the atomic density distortion associated with the dispersion force. HFKS calculations using the conventional LYP potential only generate a small distortion, giving forces significantly smaller than BD(T). The BD(T) densities have therefore been used to determine improved correlation potentials, using a modified ZMP approach; the potentials differ considerably from LYP. HFKS calculations using these potentials accurately reproduce the distortion, giving forces in good agreement with BD(T). The correlation potential has been partitioned into atomic and interaction parts. HFKS calculations using the latter generate the density distortion, giving dispersion forces essentially identical to those from the full dimer potential. The origin of this distortion can be traced to the asymmetric structure of the interaction correlation potential in the vicinity of each nucleus.

The DFT calculations in this study rely on the underlying BD(T) calculation and so do not represent a practical approach for determining dispersion forces. However, knowledge of the structure of the correlation potential at large separation may prove useful in the development of new energy functionals that correctly describe dispersion. At a more pragmatic level, they may aid the development of new model potentials or procedures for correcting existing potentials.

ACKNOWLEDGMENTS

The authors are grateful to the EPSRC for studentship support and to A. J. Stone, R. F. W. Bader, J. F. Dobson, and J. M. Hutson for helpful discussions. We are grateful to A. J. Misquitta for providing the Dc147 basis set.

[1] S. Kristyán and P. Pulay, Chem. Phys. Lett. **229**, 175 (1994).
[2] J. M. Pérez-Jordá and A. D. Becke, Chem. Phys. Lett. **233**, 134 (1995).
[3] P. Hobza, J. Šponer, and T. Reschel, J. Comput. Chem. **16**, 1315 (1995).
[4] D. C. Patton and M. R. Pederson, Phys. Rev. A **56**, R2495 (1997).
[5] Y. Zhang, W. Pan, and W. Yang, J. Chem. Phys. **107**, 7921 (1997).
[6] N. Kurita and H. Sekino, Chem. Phys. Lett. **348**, 139 (2001).
[7] X. Wu, M. C. Vargas, S. Nayak, V. Lotrich, and G. Scoles, J. Chem. Phys. **115**, 8748 (2001).
[8] C. Adamo and V. Barone, J. Chem. Phys. **108**, 664 (1998).
[9] S. Tsuzuki and H. P. Lüthi, J. Chem. Phys. **114**, 3949 (2001).
[10] J. M. Pérez-Jordá, E. San-Fabián, and A. J. Pérez-Jiménez, J. Chem. Phys. **110**, 1916 (1999).
[11] E. J. Meijer and M. Sprik, J. Chem. Phys. **105**, 8684 (1996).
[12] S. Tsuzuki, T. Uchimaru, and K. Tanabe, Chem. Phys. Lett. **287**, 202 (1998).
[13] A. Milet, T. Korona, R. Moszynski, and E. Kochanski, J. Chem. Phys. **111**, 7727 (1999).
[14] T. A. Wesolowski, J. Chem. Phys. **113**, 1666 (2000).
[15] O. Couronne and Y. Ellinger, Chem. Phys. Lett. **306**, 71 (1999).
[16] T. A. Wesolowski, O. Parisel, Y. Ellinger, and J. Weber, J. Phys. Chem. A **101**, 7818 (1997).
[17] A. K. Rappé and E. R. Bernstein, J. Phys. Chem. A **104**, 6117 (2000).
[18] A. D. Becke, Phys. Rev. A **38**, 3098 (1988).
[19] J. P. Perdew, in *Electronic Structure of Solids '91*, edited by P. Zeische and H. Eschrig (Akademie Verlag, Berlin, 1991), p. 11.
[20] J. P. Perdew, K. Burke, and M. Ernzerhof, Phys. Rev. Lett. **77**, 3865 (1996).
[21] F. A. Hamprecht, A. J. Cohen, D. J. Tozer, and N. C. Handy, J. Chem. Phys. **109**, 6264 (1998).
[22] G. Menconi, P. J. Wilson, and D. J. Tozer, J. Chem. Phys. **114**, 3958 (2001).
[23] G. Menconi and D. J. Tozer, Chem. Phys. Lett. **360**, 38 (2002).
[24] T. van Mourik and R. J. Gdanitz, J. Chem. Phys. **116**, 9620 (2002).
[25] Q. Wu and W. Yang, J. Chem. Phys. **116**, 515 (2002).
[26] E. Zaremba and W. Kohn, Phys. Rev. B **13**, 2270 (1976).
[27] K. Rapcewicz and N. W. Ashcroft, Phys. Rev. B **44**, 4032 (1991).
[28] J. F. Dobson and B. P. Dinte, Phys. Rev. Lett. **76**, 1780 (1996).
[29] Y. Andersson, D. C. Langreth, and B. I. Lundqvist, Phys. Rev. Lett. **76**, 102 (1996).
[30] E. Hult, Y. Andersson, B. I. Lundqvist, and D. C. Langreth, Phys. Rev. Lett. **77**, 2029 (1996).
[31] E. Hult, H. Rydberg, B. I. Lundqvist, and D. C. Langreth, Phys. Rev. B **59**, 4708 (1999).
[32] S. J. A. van Gisbergen, J. G. Snijders, and E. J. Baerends, J. Chem. Phys. **103**, 9347 (1995).
[33] A. G. Ioannou, S. M. Colwell, and R. D. Amos, Chem. Phys. Lett. **278**, 278 (1997).
[34] W. Kohn, Y. Meir, and D. E. Makarov, Phys. Rev. Lett. **80**, 4153 (1998).
[35] J. F. Dobson and J. Wang, Phys. Rev. Lett. **82**, 2123 (1999).
[36] M. Lein, J. F. Dobson, and E. K. U. Gross, J. Comput. Chem. **20**, 12 (1999).
[37] M. Fuchs and X. Gonze, Phys. Rev. B **65**, 235109 (2002).
[38] E. Engel, A. Höck, and R. M. Dreizler, Phys. Rev. A **61**, 032502 (2000).
[39] J. F. Dobson, D. McLennan, A. Rubio, J. Wang, T. Gould, H. M. Le, and B. P. Dinte, Aust. J. Chem. **54**, 513 (2001).

[40] H. L. Williams and C. F. Chabalowski, J. Phys. Chem. A **105**, 646 (2001).
[41] A. J. Misquitta and K. Szalewicz, Chem. Phys. Lett. **357**, 301 (2002).
[42] W. Kohn and L. J. Sham, Phys. Rev. **140**, A1133 (1965).
[43] R. G. Parr and W. Yang, *Density-Functional Theory of Atoms and Molecules* (Oxford University Press, New York, 1989).
[44] R. P. Feynman, Phys. Rev. **56**, 340 (1939).
[45] C. Lee, W. Yang, and R. G. Parr, Phys. Rev. B **37**, 785 (1988).
[46] Q. Zhao, R. C. Morrison, and R. G. Parr, Phys. Rev. A **50**, 2138 (1994).
[47] R. D. Amos *et al.*, CADPAC6.5, The Cambridge Analytic Derivatives Package, 1998.
[48] T. Korona, H. L. Williams, R. Bukowski, B. Jeziorski, and K. Szalewicz, J. Chem. Phys. **106**, 5109 (1997).
[49] G. K.-L. Chan, D. J. Tozer, and N. C. Handy, J. Chem. Phys. **107**, 1536 (1997).
[50] P. J. Wilson, T. J. Bradley, and D. J. Tozer, J. Chem. Phys. **115**, 9233 (2001).
[51] M. Levy and J. P. Perdew, in *Density Functional Methods in Physics*, edited by R. M. Dreizler and J. da Providencia (Plenum, New York, 1985), pp. 11–30.
[52] D. J. Tozer, V. E. Ingamells, and N. C. Handy, J. Chem. Phys. **105**, 9200 (1996).
[53] G. Menconi, D. J. Tozer, and S. Liu, Phys. Chem. Chem. Phys. **2**, 3739 (2000).
[54] J. O. Hirschfelder and M. A. Eliason, J. Chem. Phys. **47**, 1164 (1967).
[55] K. L. C. Hunt, J. Chem. Phys. **92**, 1180 (1990).
[56] H. Nakatsuji and T. Koga, J. Am. Chem. Soc. **96**, 6000 (1974).
[57] R. F. W. Bader and A. K. Chandra, Can. J. Chem. **46**, 953 (1968).
[58] R. F. W. Bader, *Atoms in Molecules—A Quantum Theory* (Oxford University Press, Oxford, 1990), p. 325.
[59] A. J. Stone, *The Theory of Intermolecular Forces* (Oxford University Press, Oxford, 1997), p. 81.
[60] O. V. Gritsenko, P. R. T. Schipper, and E. J. Baerends, Phys. Rev. A **57**, 3450 (1998).
[61] J. Hernández-Trujillo and R. F. W. Bader, J. Phys. Chem. A **104**, 1779 (2000).
[62] P. J. Wilson and D. J. Tozer, Chem. Phys. Lett. **337**, 341 (2001); J. Mol. Struct. **602–603**, 191 (2002).
[63] C. J. Umrigar and X. Gonze, Phys. Rev. A **50**, 3827 (1994).